International Symposium of Research Students on Materials Science and Engineering
December 20-22, Chennai, India
Department of Metallurgical and Materials Engineering, Indian Institute of Technology Madras

STRUCTURE AND EFFICIENCY OF AMINES FOR GENE DELIVERY

Heather M. Evans, A. Ahmad, K. Ewert and C. R. Safinya
Departments of Materials, Physics, and Biomolecular Science and Engineering, UCSB, Santa Barbara, CA, USA

ABSTRACT

Lipid-based systems are notoriously poor for gene delivery, and their use has been primarily empirical. In order to improve these systems, it is imperative to obtain a greater understanding of molecular interactions between DNA and positively charged molecules. We report structural studies on a range of molecules all using the same charged amine moieties, presented in three distinct morphologies: the tetravalent salt spermine, cationic dendrimers, and cationic lipids. Additionally, structures are correlated with protein expression in mammalian cells.

Keywords: Gene Therapy, Cationic Liposome, Spermine, X-ray Diffraction

1. INTRODUCTION

Despite inherent advantages over viral methods, non-viral gene delivery has met with limited success and requires further optimization. Genes are sequences of DNA that produce particular proteins within the machinery of the cell. The therapeutic benefits of delivering foreign genes hold great promise for the treatment, or perhaps even the cure, of many diseases. However, the need for better non-viral methods is underscored by setbacks of prevalent viral techniques, including the death of a patient using an adenovirus treatment[1]. The lack of a specific immune response to non-viral gene delivery methods is a major advantage, as is the unlimited capacity of DNA that can be delivered using these methods. Non-viral gene delivery methods include the use of polymers and lipids to package and deliver DNA to cells. In fact, over a quarter of current ongoing gene therapy clinical trials use non-viral methods[2]. Our research goal is the development of a sensible methodology for creating more efficient non-viral gene delivery systems, with particular attention to cationic lipids. In addition, there are unique biophysical assemblies between DNA and synthetic materials that require new physical models of self-assembly.

This paper addresses three types of cationic molecules and their interaction with DNA, with application to gene delivery. In each case the assembly of the molecules with DNA will be presented, as determined using x-ray diffraction. In the first case, the small multivalent salt spermine interacts with DNA to form condensed bundles. Spermine is found in biological systems including mammalian cells and virus assemblies and is a powerful agent for DNA compaction. The second type of cationic molecule, a dendrimer, presents a similar charged unit in a spherical morphology and we have found it to form a range of supramolecular assemblies when complexed with DNA. Finally, we introduce new cationic lipids that form another, distinct, type of assembly with DNA. Evidence of successful gene delivery using both dendrimers and lipids will be presented.

2. MATERIALS AND METHODS

2.1 Materials

Spermidine and polypropyleneimine dendrimer G4 were purchased from Sigma Aldrich and prepared in water. MVL5 was synthesized as reported[3]. 1,2-dioleoyl-sn-glycerophosphatidylcholine (DOPC) and 2,3-dioleyloxypropyltrimethylammonium chloride (DOTAP) were purchased from Avanti Polar Lipids. Liposomes were prepared from stock solutions in chloroform. These solutions were evacuated overnight and solubilized at 37 C in water, to a final concentration of 30 mM (or 0.6 mM for cell experiments). Highly polymerized calf thymus DNA was purchased from Invitrogen and solubilized to the appropriate concentration. In cell culture experiments, plasmid DNA containing the luciferase gene (pGL3 Control vector, Promega) was used.

2.2. Methods

2.2.1 X-ray diffraction

Synchrotron x-ray data was acquired at Stanford Synchrotron Radiation Laboratory using beamline 4-2. Samples were prepared using DNA at 5 mg/ml. DNA was mixed with the appropriate cation and then centrifuged at high speeds. The resulting condensates were loaded into 1.5 mm capillaries.

2.2.2 Particle Characterization

A Zeta meter was used to acquire zeta potential data. Dilute solutions of G4 dendrimer and DNA were prepared at a range of charge ratios. A Brookhaven light scattering instrument was used to quantify particle size of dilute solutions of G4 and DNA. Differential Interference Contrast (DIC) and epi-flourescence microscopy data was acquired using a Nikon Diaphot 300. Images were collected with a Nikon CoolPix camera. DNA was fluorescently labeled using Yo-Yo purchased from Molecular Probes.

2.2.3 Transfection

Mammalian fibroblast L-Cells were cultured and transfected as reported elsewhere[3]. Briefly, cells were split into 24 well plates to 80% confluency. DNA and dendrimer or DNA and liposomes were mixed in Dulbecco's Modified Eagle's Medium (Invitrogen) to a final amount of 0.4 μg DNA per well at a charge ratio (+/-) equal to 2.8, diluted in a final volume of 0.2 ml DMEM. The DNA complexes were added to the cells for 6 or 8 hours, and then aspirated. Complete media was then added for 24 hours before final aspiration. At this point, a standard luciferase protocol was used (Promega) to lyse the cells then quantify luminescence with a luminometer. Total protein was measured using the Bio-Rad protein assay as directed. Transfection efficiency was reported in relative light units per mg total protein.

3. RESULTS AND DISCUSSION

3.1 Spermine-DNA Complexes

The description of spermine and DNA is important as a foundation to the following discussions of DNA and dendrimers as well as DNA and cationic lipids. There is a known presence of polyamines within the cell, namely putrescine (2+), spermidine (3+), and spermine (4+). The specific biological function of polyamines is not entirely understood, although it is clear that their presence is critical for cellular growth, as studied by systems where there is a polyamine deficiency[4]. Polyamines have been connected with the activity of Topoisomerase I, an enzyme

that adjusts the degree of DNA coiling by cleaving one strand of the DNA helix[5]. In addition, a significant fraction of cellular polyamines interact with RNA, inducing structural changes and stimulating protein synthesis, as well as nucleotide triphosphotases and proteins. Igarashi and Kashiwagi estimated the molarity of polyamines present in various types of cells, in ranges of 1.33 – 6.88 mM spermidine and 1.58 –0.88 mM spermine[6].

Spermine is a 4+ multivalent molecule whose charged units are amino groups. In aqueous solution, these groups become protonated and form the molecule shown in figure 1. Although DNA is highly negatively charged, rods of DNA condense into bundles in the presence of spermine. This is thought to be partially due to the renormalization of DNA charge that occurs due to counterion condensation, resulting in tightly bound sodium (1+) counterions along the helical DNA backbone[7, 8]. Furthermore, the replacement of three sodium counterions by one tetravalent spermine molecule will increase the entropy of the system by releasing four molecules in exchange for the "entrapment" of a single spermine molecule, and it is empirically known that counterions of charge greater than 2+ can condense DNA. There is much interest in the physical description of the mechanism for the attraction of two similarly charged DNA rods; simple electrostatic predictions fail and short range attractions and long wavelength fluctations are required to predict this like charged attraction phenomenon[9, 10].

In dilute solutions, intra-strand DNA condensation can be seen in the shape of toroids and rods with local hexagonal packing and can be imaged using, for example, atomic force or electron microscopy[11]. Figure 1 shows x-ray diffraction of more concentrated DNA – spermine condensates, which agree with results published by other researchers[12]. In this case, a peak at q = 0.241 $Å^{-1}$ corresponds to hexagonal packing within DNA having a real space inter-DNA distance a = 3.0 nm, since $a = 4\pi/\sqrt{3}q_0$ for hexagonal lattices. The affinity of spermine for DNA may also include specific molecular details of the DNA double helix structure. Stereospecific interactions between DNA and polyamines were predicted by Liquori et al using the crystal structure of spermine, and the proposed interactions between the cationic molecules and the narrow groove of DNA include hydrogen bonding, electrostatic interactions, and hydrophobic bonding[13].

3.2 Dendrimer-DNA Complexes

Dendrimers represent a new class of synthetic molecules, created in a branched synthesis leading to spherical particles rather than linear polymeric chains. Cationic polypropylene-imine (PPI) dendrimers consist of building blocks of spermidine-like units, with charged groups again made up of protonated amines. This type of charged group is also present in the polymer polyethyleneimine, which has been explored as a vehicle for gene delivery due to its ability to condense and deliver DNA to cells[14]. In this paper we present structure and function results from generation 4 PPI. The structure of this molecule is shown in figure 2. While there is no conclusive data, current research indicates that polybasic dendrimers such as PPI have a homogeneous density distribution and therefore backfold in solution rather than fully extend, although steric hindrance between charged amines is an important consideration[15, 16]. The branched structure of G4 has 62 total amino groups, although it is likely that some of these are unavailable for protonation due to the density of the molecule and backfolding that is anticipated. According to Topp et al, the radius of gyration for G4 PPI is $R_g^+ = 12.4 \pm 0.2$ Å, resulting in a radius in dilute solution of 16 Å calculated using the relationship $R^2 = (5/3)(R_g^{+2})$[17].

Characterization of PPI-DNA complexes is shown in figure 3. A parameter P/D defines the overall charge of the complexes; i.e. P/D indicates equivalent charges due to PPI and DNA. Zeta-potential measurements quantify the surface charge of PPI-DNA complexes. These results

(figure 3a) are shown in terms of the charge ratio P/D using a charge of 36+ for the G4 molecules, which gives a good fit to the charge neutral point of the PPI-DNA complexes measured by zeta potential. This value is less than the 62 available amino groups within the structure but is consistent with our expectations that not all of the amines are fully charged. For values below P/D = 1, the complexes are negatively charged since there is an excess of negative charges from DNA. Similarly, for values above P/D = 1, the complexes are positively charged due to an excess of cationic dendrimer charge. These results are reminiscent of studies using liposomes to condense DNA, in which the complexes become undercharged or overcharged, either below or above the charge neutral point, respectively[18].

Dynamic light scattering results (figure 3b) indicate a PPI-DNA complex size of around 200 nm for all values of P/D. Parallel experiments using optical and epi-fluorescent microscopy shown in figure 3c illustrate these complexes at P/D = 4. The DNA is dyed with a fluorescent label and appears to correspond to the particles imaged using differential interference contrast, although it is not possible to identify identical particles between the two micrographs, since the particles are moving quickly in aqueous solution.

X-ray diffraction (Figure 4) reveals three distinct phases of PPI-DNA complexes[19]. At low P/D, less than one, there is a single diffraction peak at q = 0.22 Å (fig. 4a). The position and characteristic of this feature is similar to results obtained with the multivalent salt spermine, which indicates that the mechanism of DNA binding for dendrimers may be the same as for spermine. At higher charge ratios, $1 \leq P/D \leq 2.5$, x-ray diffraction results show a square phase (fig. 4b). This is indicated by two diffraction peaks q_0 and q_1 where $q_1 = \sqrt{2}q_0$. The real space lattice constant of a = 35 Å of this phase is given by $a = 2\pi/q_0$. This phase is a local organization of DNA rods held together by dendrimers, with the cross-section of DNA molecules in a square lattice (fig. 4d). Surprisingly, a new phase is encountered at P/D ratios > 2.5. In this case, the two diffraction peaks are related by $q_1 = \sqrt{3}q_0$, which gives a real space lattice constant a = 43 Å according to the relationship $a = 4\pi/\sqrt{3}q_0$ (fig. 4c). In Phase III the DNA rods are organized into a hexagonal lattice, again held together by dendrimers (fig. 4e). If more dendrimers have packed into the PPI-DNA complex at higher P/D, then steric constraints and dendrimer-dendrimer repulsion would predict the larger DNA spacing given by x-ray diffraction. We developed a model to describe these phase transitions[19].

Ultimately, our interests lie in the development of vehicles for gene delivery. To this end, we used G4 dendrimers to condense plasmid DNA for delivery to cultured mammalian cells. The process of DNA delivery to cells and subsequent translation of the DNA into a protein is referred to as transfection. Plasmid DNA containing the gene for luciferase is used for our transfection experiments. Luciferase production is quantified in terms of relative light units (RLU) and is normalized to the total amount of protein present. The transfection results in figure 3d show a dramatic increase in transfection efficiency as P/D increases beyond a value of one; an overall positive PPI-DNA complex charge is required for maximum efficiency. This is consistent with our assumption that a positively charged complex is more likely to adsorb onto the negatively charged cellular surface[20]. In coordination with the phases identified using x-ray diffraction, it appears that phases II and III both lead to high efficiency.

3.3 Multivalent Lipids

Cationic liposomes are one of the prominent methods for non-viral gene delivery. Liposomes consist of lipids, which are amphiphilic molecules with a hydrophobic region (consisting of carbon tails) and a hydrophilic headgroup. These molecules arrange into vesicles, resembling thin-shelled spheres. In this paper we will review some preliminary results with a new cationic lipid, MVL5, whose synthesis was developed in our lab and reported elsewhere[3]. In fact, a

series of multivalent lipids ranging from 1 to 5+ has been synthesized and is discussed in recent papers[21, 22]. The lipid headgroups consist of amino groups that are structurally reminiscent of spermine, in which the cationic charge is brought about by protonation in water. The results given herein use the largest of these lipids, MVL5, which has a headgroup charge of 5+ and is shown in figure 5. It is typical to mix cationic lipids with neutral lipids to create liposomes that consist of a ratio of the two lipids. DOPC is a standard neutral lipid used for this purpose, and results hereafter include DOPC mixed with MVL5.

The liposomes and DNA assemble into a different structure than that described in the dendrimer section of this paper. The majority of liposome-DNA mixtures form a lamellar phase, L_α^c, consisting of onion-like lipid bilayers with DNA in between. Our lab initially reported this structure, as formed with a conventional cationic lipid, DOTAP, and neutral DOPC[23]. A schematic of this is shown in figure 6a, and the characteristic distances acquired by x-ray diffraction are labeled. Figure 6b shows x-ray data for MVL5/DOPC (30% / 70% by mol%) liposomes mixed with DNA. Narrow, intense peaks labeled q_0, q_1, and q_2 correspond to the lamellar repeat distance of one lipid bilayer (δ_m) plus one layer of water (δ_w), with the relationships $q_1 = 2q_0$ and $q_2 = 3q_0$. This gives a real space repeat distance $d = \delta_m + \delta_w = 70$ Å (given by $2\pi/q_0$). A broader peak labeled q_{DNA} corresponds to the inter-DNA spacing within the lipid bilayers. The DNA-DNA spacing is $d_{DNA} = 27$ Å, given by $2\pi/q_{DNA}$. This value is remarkably small, considering that the effective diameter of DNA is about 2.5 nm in water[24]. The MVL5 headgroup condenses DNA in two dimensions so that the DNA rods are nearly touching one another. We attribute this in part to unique affinity of the spermine-like headgroup with DNA, similar to the other cases described in this paper.

MVL5/DOPC liposomes can be used to successfully deliver DNA to cells. An example of this trend is shown in Figure 6c. In this case, we compare the efficiency of MVL5/DOPC liposomes with a control system using commercially available (monovalent) DOTAP. At equivalent molar ratios of cationic lipid, MVL5 surpasses the efficiency of the control system. In fact, at 20 mol% cationic lipid, MVL5 results in efficiencies over *1000 times higher* than the control system using DOTAP. Results for the entire MVL series, and a model identifying membrane charge density as a critical parameter, are elaborated elsewhere[21].

4. CONCLUSIONS

In this paper we demonstrate three distinct methods of condensing DNA. In the first case, the small molecule spermine is used to bundle DNA. This behavior is quantified using x-ray diffraction. The same technique illuminates three distinct phases that occur using more highly charged spheres of cationic charge, dendrimer G4. These molecules are also used to deliver DNA to cells. Finally, a new series of multivalent lipids lead to different assemblies with DNA and show great promise for new gene delivery vehicles. All three systems distinctly interact with DNA, but in each case the unique phases seen may benefit from specific interactions between protonated amino groups with DNA.

5. ACKNOWLEDGEMENTS

This work was funded by the National Institutes of Health (NIH GM-59288) and the National Science Foundation (DMR 0203755). The Stanford Synchrotron Radiation Facility is operated under the United States Department of Energy. Heather Evans thanks the National Science Foundation for a Graduate Research Fellowship.

6. REFERENCES

1. Raper, S. E., Chirmule, N., Lee, F. S., Wivel, N. A., Bagg, A., Gao, G. P., Wilson, J. M. & Batshaw, M. L. *Molecular Genetics and Metabolism* **80** (2003) 148.
2. http://www.wiley.co.uk/genetherapy/clinical/.
3. Ewert, K., Ahmad, A., Evans, H. M., Schmidt, H.-W. & Safinya, C. R. *Journal of Medicinal Chemistry* **45** (2002) 5023.
4. Tabor, C. W. & Tabor, H. *Annual Reviews in Biochemistry* **53** (1984) 749.
5. Sukhanova, A., Devy, J., Pluot, M., Bradley, J.-C., Vigneron, J.-P., Jardillier, J.-C., Lehn, J.-M. & Nabiev, I. *Bioorganic and Medicinal Chemistry* **9** (2001) 1255.
6. Igarashi, K. & Kashiwago, K. *Biochemical and Biophysical Research Communications* **271** (2000) 559.
7. Manning, G. S. *Quarterly Reviews of Biophysics* **11** (1978) 179.
8. Manning, G. S. *Journal of Chemical Physics* **51** (1969) 924.
9. Gronbech-Jensen, N., Mashl, R. J., Bruinsma, R. F. & Gelbart, W. M. *Physical Review Letters* **78** (1997) 2477.
10. Gelbart, W. M., Bruinsma, R. F., Pincus, P. & Parsegian, V. A. *Physics Today* **53** (2000) 38.
11. Bloomfield, V. *Nucleic Acid Science* **44** (1998) 269.
12. Raspaud, E., M., de la Cruz, O., Sikorav, J.-L. & Livolant, F. *Biophysical Journal* **74** (1998) 381.
13. Costanti, L., Crescenz, V., Elia, V., Giglio, E., Puliti, R., Desantis, M. & Vitaglia, V. *Journal of Molecular Biology* **24** (1967) 113.
14. Kichler, A., Behr, J.-P. & Erbacher, P. in *Nonviral Vectors for Gene Therapy*, eds. Haung, L., Hung, M.-C. & Wagner, E. Academic Press, San Diego, (1999) p. 192.
15. Bosman, A. W., Jannsen, H. M. & Meijer, E. W. *Chemical Reviews* **99** (1999) 1665.
16. Ramzi, A., Scherrenberg, R., Brackman, J., Joosten, J. & Mortensen, K. *Macromolecules* **31** (1998) 1621.
17. Topp, A., Bauer, B. J., Prosa, T. J., Scherrenberg, R. & Amis, E. J. *Macromolecules* **32** (1998) 8923.
18. Koltover, I., Salditt, T. & Safinya, C. R. *Biophysical Journal* **77** (1999) 915.
19. Evans, H. M., Ahmad, A., Ewert, K., Pfohl, T., Martin-Herranz, A., Bruinsma, R. F. & Safinya, C. R. *Physical Review Letters* **91** (2003) 075501.
20. Lin, A. J., Slack, N. L., Ahmad, A., George, C. X., Samuel, C. S. & Safinya, C. R. *Biophysical Journal* **84** (2003) 3307.
21. Ahmad, A., Evans, H. M., Ewert, K., George, C. X., Samuel, C. S. & Safinya, C. R. *Journal of Gene Medicine, accepted* (2004).
22. Ewert, K., Slack, N. L., Ahmad, A., Evans, H. M., Lin, A. J., Samuel, C. S. & Safinya, C. R. *Current Medicinal Chemistry* **11** (2004) 133.
23. Radler, J. O., Koltover, I., Salditt, T. & Safinya, C. R. *Science* **275** (1997) 810.
24. Podgornik, R., Rau, D. C. & Parsegian, V. A. *Macromolecules* **22** (1989) 1780.

FIGURES

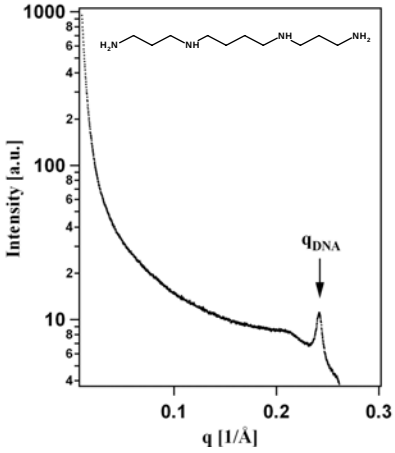

Figure 1. X-ray scan of 10 mM Spermine complexed with DNA. The DNA correlation peak is labeled q_{DNA}. The structure of spermine is shown at the top, inset.

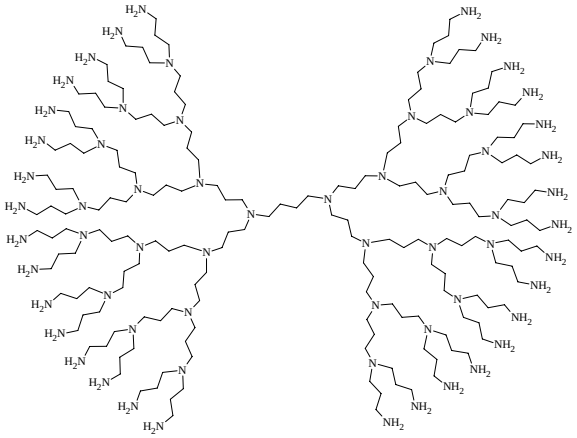

Figure 2. Structure of dendrimer G4.

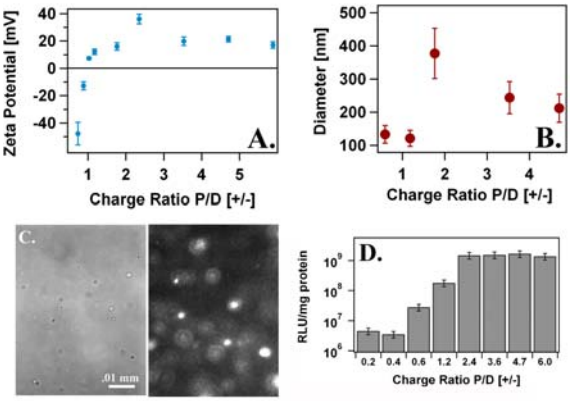

Figure 3. Particle zeta potential, equivalent to surface charge, vs. charge ratio, P/D, is shown in (a). Particle size measurements in (b) show that the diameter of G4-DNA complexes is on the order of 200 nm. Microscopy in (c) shows DIC mode (left) and DNA fluorescence mode (right) for P/D = 4 complexes. Transfection results with cells (d) indicate higher efficiency for P/D > 1 (positively charged complexes).

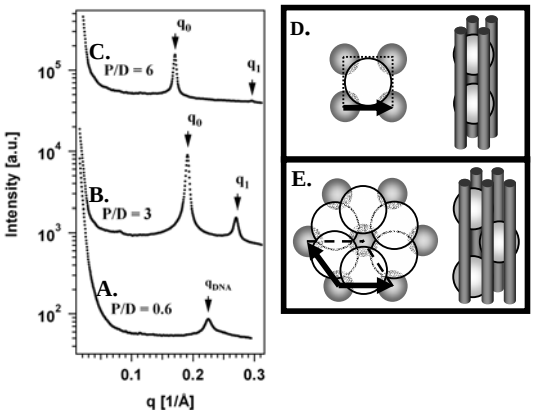

Figure 4. X-ray diffraction results for G4-DNA complexes. In (a), a single peak similar to sperimine results is seen for low P/D values. In (b), a square phase is seen (illustrated in (d)). In (c), a hexagonal phase (drawn in e) is detected for highest P/D values. Modified from ref. 19.

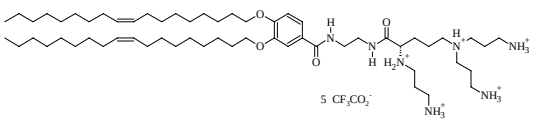

Figure 5. Molecular Structure of MVL5.

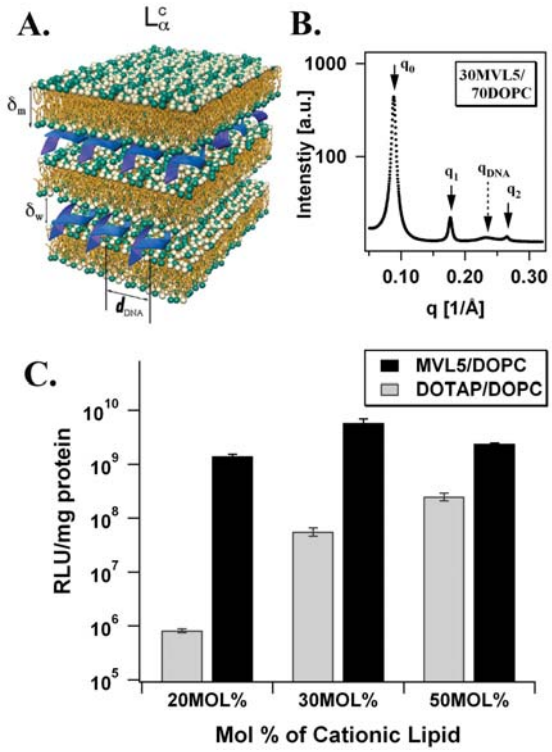

Figure 6. In (a), a schematic of the lamellar phase is shown. A typical x-ray scan for MVL5/DOPC and DNA complexes is shown in (b) where peaks corresponding to lipid bilayer repeats are marked with solid arrow, and dashed arrow denotes the intralayer DNA correlation peak. Transfection efficiency (c) shows higher efficiency compared to a control DOTAP system for all three different mol % of cationic lipid. Modified from ref. 3.